Models for Bimetallic Catalysis: Selectivity in Ligand Addition to a Coordinatively Unsaturated Pt_3Re Cluster Cation

Jianliang Xiao, Leijun Hao, and Richard J. Puddephatt*

Department of Chemistry, University of Western Ontario, London, Canada N6A 5B7

Ljubica Manojlović-Muir,* Kenneth W. Muir, and Ali Ashgar Torabi

Department of Chemistry, University of Glasgow, Glasgow, Scotland G12 8QQ

Received April 19, 1995[⊗]

The coordinatively unsaturated, 54-electron Pt_3Re cluster cation $[Pt_3\{Re(CO)_3\}(\mu\text{-dppm})_3]^+$, **2**, dppm = $Ph_2PCH_2PPh_2$, reacts with ligands L = $P(OR)_3$, CO, RNC, RSH or RC≡CH to give the 56-electron cluster cations $[Pt_3\{Re(CO)_3L\}(\mu\text{-dppm})_3]^+$ by selective addition to the rhenium center, in contrast to the known addition of these ligands to the Pt_3 center in $[Pt_3(\mu_3\text{-CO})(\mu\text{-dppm})_3]^{2+}$. The reaction with CO is easily reversible. The complex with L = $P(OPh)_3$ has been characterized by an X-ray structure determination $\{[Pt_3\{Re(CO)_3L\}(\mu\text{-dppm})_3][PF_6]\cdot EtOH$; triclinic, $P\bar{1}$, a = 13.993(1) Å, b = 17.868(1) Å, c = 19.753(2) Å, α = 88.198(7)°, β = 87.766(7)°, γ = 72.394(4)°, V = 4702.9(7) Å^3, Z = 2, R = 0.0405, R_w = 0.0429 for 14 765 unique reflections with $I > 3\sigma(I)\}$. The structure contains a distorted tetrahedral Pt_3Re core with the Pt_3 triangle edge-bridged by three μ-dppm ligands, the two PtRe edges weakly semibridged by CO ligands, and the phosphite ligand bound to rhenium [Pt–Pt = 2.603(1)–2.677(1) Å, Pt–Re = 2.762(1)–2.942(1) Å]. NMR studies indicate that several of the adducts are fluxional, by rotation of the $Re(CO)_3L$ fragment about the Pt_3 triangle, such that they appear to have C_3 symmetry. Phosphite ligands displace CO or HCCH from $[Pt_3\{Re(CO)_4\}(\mu\text{-dppm})_3]^+$ or $[Pt_3\{Re(CO)_3(HCCH)\}(\mu\text{-dppm})_3]^+$, respectively, to give $[Pt_3\{Re(CO)_3P(OR)_3\}(\mu\text{-dppm})_3]^+$. The clusters are considered to be formed by donation of electron pairs from the Pt–Pt bonding orbitals of a $Pt_3(\mu\text{-dppm})_3$ fragment to acceptor orbitals of the $Re(CO)_3$ or $Re(CO)_3L$ unit; Pt–Re bonding is therefore weaker in the 56-electron clusters. An analogy is noted between the donor orbitals of the $Pt_3(\mu\text{-dppm})_3$ fragment and of $C_5H_5^-$, which is useful in interpreting the chemistry. The observation of selective reactivity at rhenium is relevant to the mode of action of heterogeneous Pt/Re catalysts.

Introduction

Heteronuclear transition metal cluster complexes have fascinating properties and are of particular interest as models for heterogeneous bimetallic alloy catalysts.[1,2] One of the most important of such catalysts is the $Pt/Re/Al_2O_3$ system used in catalytic reforming of petroleum.[3] As a result of this interest, several binuclear and cluster complexes containing Pt–Re bonds have been synthesized and structurally characterized and can serve as models for the metal–metal-bonded units which may be present in the bimetallic catalysts.[4] However, there have been few studies of the chemical reactivity of Pt–Re-bonded complexes.[1,4,5] In order to model the reactivity of a bimetallic catalyst compared to a simple platinum catalyst, it would be useful to study the reactivity of a coordinatively unsaturated Pt–Re cluster compared to a simple Pt cluster. This is now possible with clusters based on the $Pt_3(\mu\text{-dppm})_3$ triangle, dppm = $Ph_2PCH_2PPh_2$, since both cluster cations $[Pt_3(\mu_3\text{-CO})(\mu\text{-dppm})_3]^{2+}$, **1**,[6] and $[Pt_3\{\mu_3\text{-Re}(CO)_3\}(\mu\text{-dppm})_3]^+$, **2**,[5] are now known. The complex cations **1** and **2** have 42- and 54-electron configurations, respec-

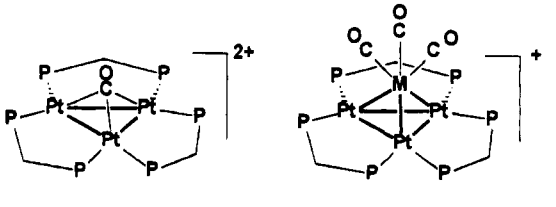

1 **2, M = Re; 3, M = Mn**

[⊗] Abstract published in *Advance ACS Abstracts,* August 1, 1995.

(1) (a) Adams, R. D.; Wu, W. *Organometallics* **1993**, *12*, 1238; 1248. (b) Churchill, M. R.; Lake, C. H.; Safarowic, F. J.; Parfitt, D. S.; Nevinger, L. R.; Keister, J. B. *Organometallics* **1993**, *12*, 671. (c) Song, L. C.; Shen, J. Y.; Hu, Q. M.; Wang, R. J.; Wang, H. G. *Organometallics* **1993**, *12*, 408. (d) Adams, R. D.; Li, Z.; Swepston, P.; Wu, W.; Yamamoto, J. *J. Am. Chem. Soc.* **1992**, *114*, 10657. (e) Farrugia, L. J. *Adv. Organomet. Chem.* **1990**, *31*, 301.

(2) Adams, R. D.; Herrmann, W. A. *Polyhedron* **1988**, *7*, 2255–2464.

(3) Biswas, J.; Bickle, G. M.; Gray, P. G.; Do, D. D.; Barbier, J. *Catal. Rev. Sci. Eng.* **1988**, *30*, 161.

(4) (a) Xiao, J.; Vittal, J. J.; Puddephatt, R. J. *J. Chem. Soc., Chem. Commun.* **1993**, 167. (b) Beringhelli, T.; Ceriotti, A.; Ciani, G.; D'Alfonso, G.; Garlaschelli, L.; Pergola, R. D.; Moret, M.; Sironi, A. *J. Chem. Soc., Dalton Trans.* **1993**, 199. (c) Antognazza, P.; Beringhelli, T.; D'Alfonso, G.; Minoja, A.; Ciani, G.; Moret, M.; Sironi,A. *Organometallics* **1992**, *11*, 1777. (d) Powell, J.; Brewer, J. C.; Gulia, G.; Sawyer, J. F. *J. Chem. Soc., Dalton Trans.* **1992**, 2503. (e) Beringhelli, T.; D'Alfonso, G.; Minoja, A. P. *Organometallics* **1991**, *10*, 394. (f) Ciani, G.; Moret, M.; Sironi, A.; Antognazza, P.; Beringhelli, T.; D'Alfonso, G.; Pergola, R. D.; Minoja, A. *J. Chem. Soc., Chem. Commun.* **1991**, 1255. (g) Ciani, G.; Moret, M.; Sironi, A.; Beringhelli, T.; D'Alfonso, G.; Pergola, R. D. *J. Chem. Soc., Chem. Commun.* **1990**, 1668. (h) Beringhelli, T.; Ceriotti, A.; D'Alfonso, G.; Pergola, R. D. *Organometallics* **1990**, *9*, 1053. (i) Carr, S. W.; Fontaine, X. L. R.; Shaw, B. L.; Thornton-Pett, M. *J. Chem. Soc., Dalton Trans.* **1988**, 769.

0276-7333/95/2314-4183$09.00/0

tively, and so each is coordinatively unsaturated (the common electron counts for trinuclear and tetranuclear clusters are 48 and 60, respectively).[7] In heteronuclear clusters containing platinum, the coordinative unsaturation is normally localized at the platinum, which commonly has a 16-electron configuration in mononuclear, binuclear, and cluster complexes.[7] Of course, the complex cation **1** can only react at platinum, but previous work on mixed platinum/main group metal clusters, such as those containing $Pt_3(\mu_3\text{-}SnX_3)$ or $Pt_3(\mu_3\text{-}Hg)$ units, has shown that ligands add selectively to platinum as expected, sometimes with displacement of the main group metal.[8,9] It is therefore particularly interesting that neutral donor ligands react with complex **2** at rhenium and not at one or more of the platinum centers,[10] while anionic ligands such as I^- add to the Pt_3 triangle.[11] This article reports details of the neutral ligand addition reactions to **2** and, to a lesser extent, to the corresponding manganese cluster $[Pt_3\{\mu_3\text{-}Mn(CO)_3\}(\mu\text{-dppm})_3]^+$, **3**, using the reagents CO, RNC, $P(OR)_3$, RSH, and RC≡CH. Previous communications have reported the synthesis of **2** and **3** and the unique reactions of **2** with oxygen and sulfur donors.[5]

Results

It will be seen that the ligand addition reactions are much better defined with the rhenium cluster **2** than with the manganese analog **3**. The reactions with phosphite ligands, carbon monoxide, and alkynes will be described in that order.

Reactions with Phosphite Ligands. Phosphite ligands reacted rapidly with cluster **2** to give the adducts $[Pt_3\{Re(CO)_3L\}(\mu\text{-dppm})_3]^+$, [**4**, L = $P(OMe)_3$; **5**, L = $P(OPh)_3$] according to eq 1. These complexes, as the

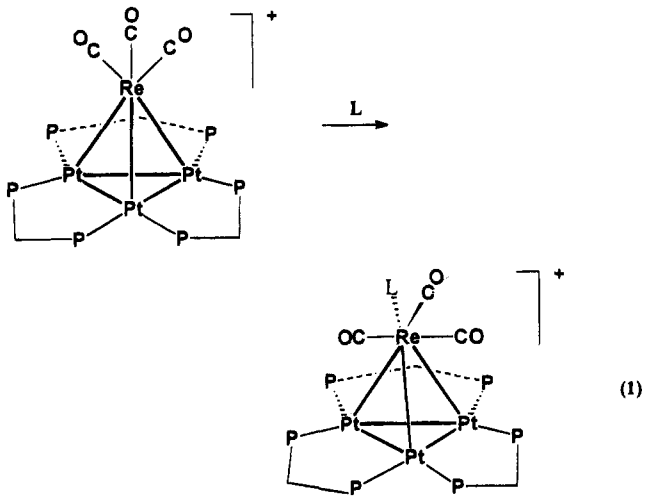

(1)

4, L = $P(OMe)_3$ **10**, L = XyNC
5, L = $P(OPh)_3$ **11**, L = EtSH
6, L = CO **12**, L = *t*-BuSH
7, L = MeNC **13**, L = 3-MeC_6H_4SH
8, L = *t*-BuNC **14**, L = HCCH
9, L = CyNC **15**, L = PhCCH

$[PF_6]^-$ salts, are dark brown solids; they are stable to air at room temperature, and they do not easily undergo ligand dissociation of either a carbonyl or the phosphite ligand. It is important to note that **1** reacts with these ligands in a completely different way, namely by addition to platinum as shown in eq 2.[8,12]

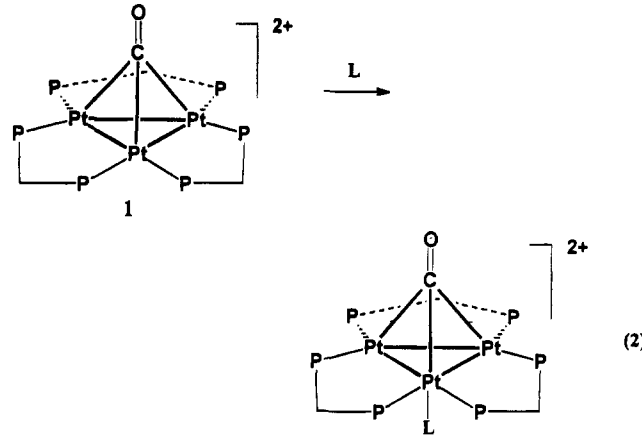

(2)

Complex **5** was characterized by an X-ray structure analysis of **5**$[PF_6]$·EtOH. Selected bond lengths and angles are listed in Table 1. The molecular structure of **5**, presented in Figure 1, shows that addition of the phosphite ligand to **2** occurs selectively at the rhenium center.

The structure is built of $Re(CO)_3\{P(OPh)_3\}^+$ and $Pt_3(\mu\text{-dppm})_3$ fragments. The Pt_3 triangle is capped by the $Re(CO)_3\{P(OPh)_3\}^+$ fragment to form a distorted tetrahedral Pt_3Re cluster with two edges, Pt(1)–Re and Pt(2)–Re, weakly semibridged by carbonyl ligands [Re–C = 1.969(9), 1.998(9) Å; Pt–C = 2.428(9), 2.550(9) Å; Re–C–O = 171.4(8), 170.6(8)°]. The $Pt_3Re(CO)_3(PO_3)(\mu\text{-PCP})_3$ core approximates C_s symmetry (Figure 2), with the mirror plane passing through the Pt(3), Re, P(7), C(1), and C(4) atoms and bisecting the Pt(1)–Pt(2) bond. Distorted octahedral geometry about the Re atom in the $Re(CO)_3\{P(OPh)_3\}^+$ unit, evident from the bond angles shown in Table 1, is completed by the Pt(3) atom and the midpoint of the Pt(1)–Pt(2) bond.

In **5**, the Pt–Pt bonds show small variations [2.603(1), 2.635(1), 2.677(1) Å]. Variations in the Pt–Re distances are larger [2.762(1), 2.825(1), 2.942(1) Å], but all three distances lie within the accepted range of 2.65–3.00 Å.[4,5,10,11] The average Pt–Pt (2.60 Å in **2**, 2.64 Å in **5**) and Pt–Re (2.67 Å in **2**, 2.84 Å in **5**) distances indicate that the phosphite addition occurs at the expense of metal–metal bonding, with the Pt–Re bonds weakened more than the Pt–Pt bonds.

(5) (a) Xiao, J.; Vittal, J. J.; Puddephatt, R. J.; Manojlović-Muir, Lj.; Muir, K. W. *J. Am. Chem. Soc.* **1993**, *115*, 7882. (b) Hao, L.; Xiao, J.; Vittal, J. J.; Puddephatt, R. J. *J. Chem. Soc., Chem. Commun.* **1994**, 2183.

(6) Ferguson, G.; Lloyd, B. R.; Puddephatt, R. J. *Organometallics* **1986**, *5*, 344.

(7) Mingos, D. M. P.; May, A. S. In *The Chemistry of Metal Cluster Complexes*: Shriver, D. F., Kaesz, H. D., Adams, R. D., Eds.; VCH: New York, 1990. The most common electron count for tetrahedral clusters is 60, such as in $[Ir_4(CO)_{12}]$.

(8) Puddephatt, R. J.; Manojlović-Muir, Lj.; Muir, K. W. *Polyhedron* **1990**, *9*, 2767.

(9) (a) Jennings, M. C.; Schoettel, G.; Roy, S.; Puddephatt, R. J.; Douglas, G.; Manojlović-Muir, Lj.; Muir, K. W. *Organometallics* **1991**, *10*, 580. (b) Schoettel, G.; Vittal, J. J.; Puddephatt, R. J. *J. Am. Chem. Soc.* **1990**, *112*, 6400. (c) Payne, N. C.; Ramachandran, R.; Schoettel, G.; Vittal, J. J.; Puddephatt, R. J. *Inorg. Chem.* **1991**, *30*, 4048.

(10) Xiao, J.; Hao, L.; Puddephatt, R. J.; Manojlović-Muir, Lj.; Muir, K. W.; Torabi, A. A. *J. Chem. Soc., Chem. Commun.* **1994**, 2221.

(11) Xiao, J.; Hao, L.; Puddephatt, R. J.; Manojlović-Muir, Lj.; Muir, K. W.; Torabi, A. A. *Organometallics*, **1995**, *14*, 2194.

(12) (a) Bradford, A. M.; Douglas, G.; Manojlović-Muir, Lj.; Muir, K. W.; Puddephatt, R. J. *Organometallics* **1990**, *9*, 409. (b) Bradford, A. M.; Kristof, E.; Rashidi, M.; Yang, D.-S.; Payne, N. C.; Puddephatt, R. J. *Inorg. Chem.* **1994**, *33*, 2355. (c) Jennings, M. C.; Payne, N. C.; Puddephatt, R. J. *Inorg. Chem.* **1987**, *26*, 3776.

Table 1. Selected Interatomic Distances (Å) and Angles (deg)

Pt(1)–Pt(2)	2.677(1)	Pt(1)–Pt(3)	2.635(1)	P(1)–C(1)	1.851(8)	P(2)–C(1)	1.863(8)
Pt(1)–Re	2.825(1)	Pt(1)–P(2)	2.298(2)	P(3)–C(2)	1.869(8)	P(4)–C(2)	1.840(8)
Pt(1)–P(5)	2.253(3)	Pt(1)–C(6)	2.550(9)	P(5)–C(3)	1.858(9)	P(6)–C(3)	1.846(8)
Pt(2)–Pt(3)	2.603(1)	Pt(2)–Re	2.762(1)	P(7)–O(1)	1.598(6)	P(7)–O(2)	1.623(6)
Pt(2)–P(1)	2.268(3)	Pt(2)–P(4)	2.289(3)	P(7)–O(3)	1.625(6)	O(1)–C(G1)	1.410(11)
Pt(2)–C(5)	2.428(9)	Pt(3)–Re	2.942(1)	O(2)–C(H1)	1.373(10)	O(3)–C(I1)	1.388(9)
Pt(3)–P(3)	2.307(2)	Pt(3)–P(6)	2.281(3)	O(4)–C(4)	1.149(12)	O(5)–C(5)	1.150(11)
Re–P(7)	2.255(3)	Re–C(4)	1.885(10)	O(6)–C(6)	1.147(11)		
Re–C(5)	1.998(9)	Re–C(6)	1.969(9)				

Pt(2)–Pt(1)–Pt(3)	58.7(1)	Pt(2)–Pt(1)–Re	60.2(1)	C(4)–Re–C(5)	90.5(4)	C(4)–Re–C(6)	89.9(4)
Pt(2)–Pt(1)–P(2)	96.6(1)	Pt(2)–Pt(1)–P(5)	142.0(1)	C(5)–Re–C(6)	175.5(4)	Pt(2)–P(1)–C(1)	111.1(3)
Pt(2)–Pt(1)–C(6)	102.7(2)	Pt(3)–Pt(1)–Re	65.1(1)	Pt(2)–P(1)–C(E1)	111.7(4)	Pt(2)–P(1)–C(F1)	121.0(3)
Pt(3)–Pt(1)–P(2)	155.1(1)	Pt(3)–Pt(1)–P(5)	91.9(1)	C(1)–P(1)–C(E1)	106.7(5)	C(1)–P(1)–C(F1)	98.2(5)
Pt(3)–Pt(1)–C(6)	88.1(2)	Re–Pt(1)–P(2)	107.3(1)	C(E1)–P(1)–C(F1)	106.6(5)	Pt(1)–P(2)–C(1)	108.8(3)
Re–Pt(1)–P(5)	132.2(1)	Re–Pt(1)–C(6)	42.6(2)	Pt(1)–P(2)–C(C1)	122.2(3)	Pt(1)–P(2)–C(D1)	115.7(3)
P(2)–Pt(1)–P(5)	108.6(1)	P(2)–Pt(1)–C(6)	101.8(3)	C(1)–P(2)–C(C1)	101.9(4)	C(1)–P(2)–C(D1)	103.2(4)
P(5)–Pt(1)–C(6)	99.4(3)	Pt(1)–Pt(2)–Pt(3)	59.8(1)	C(C1)–P(2)–C(D1)	102.8(5)	Pt(3)–P(3)–C(2)	113.5(3)
Pt(1)–Pt(2)–Re	62.6(1)	Pt(1)–Pt(2)–P(1)	93.5(1)	Pt(3)–P(3)–C(K1)	118.1(4)	Pt(3)–P(3)–C(M1)	115.9(3)
Pt(1)–Pt(2)–P(4)	139.0(1)	Pt(1)–Pt(2)–C(5)	107.0(3)	C(2)–P(3)–C(K1)	104.5(5)	C(2)–P(3)–C(M1)	101.2(4)
Pt(3)–Pt(2)–Re	66.4(1)	Pt(3)–Pt(2)–P(1)	152.3(1)	C(K1)–P(3)–C(M1)	101.4(4)	Pt(2)–P(4)–C(2)	109.1(3)
Pt(3)–Pt(2)–P(4)	92.0(1)	Pt(3)–Pt(2)–C(5)	83.6(3)	Pt(2)–P(4)–C(J1)	115.6(4)	Pt(2)–P(4)–C(L1)	120.0(4)
Re–Pt(2)–P(1)	109.7(1)	Re–Pt(2)–P(4)	136.3(1)	C(2)–P(4)–C(J1)	103.0(4)	C(2)–P(4)–C(L1)	101.7(4)
Re–Pt(2)–C(5)	44.7(3)	P(1)–Pt(2)–P(4)	106.1(1)	C(J1)–P(4)–C(L1)	105.2(5)	Pt(1)–P(5)–C(3)	108.0(3)
P(1)–Pt(2)–C(5)	113.5(3)	P(4)–Pt(2)–C(5)	97.8(3)	Pt(1)–P(5)–C(N1)	119.4(4)	Pt(1)–P(5)–C(O1)	118.7(4)
Pt(1)–Pt(3)–Pt(2)	61.5(1)	Pt(1)–Pt(3)–Re	60.6(1)	C(3)–P(5)–C(N1)	103.7(4)	C(3)–P(5)–C(O1)	102.8(4)
Pt(1)–Pt(3)–P(3)	155.1(1)	Pt(1)–Pt(3)–P(6)	94.8(1)	C(N1)–P(5)–C(O1)	102.2(5)	Pt(3)–P(6)–C(3)	112.2(3)
Pt(2)–Pt(3)–Re	59.4(1)	Pt(2)–Pt(3)–P(3)	93.8(1)	Pt(3)–P(6)–C(A1)	120.8(4)	Pt(3)(–P(6)–C(B1)	113.1(3)
P5(2)–Pt(3)–P(6)	155.6(1)	Re–Pt(3)–P(3)	110.2(1)	C(3)–P(6)–C(A1)	101.6(5)	C(3)–P(6)–C(B1)	101.3(4)
Re–Pt(3)–P(6)	115.6(1)	P(3)–Pt(3)–P(6)	109.6(1)	C(A1)–P(6)–C(B1)	105.7(4)	Re–P(7)–O(1)	113.9(3)
Pt(1)–Re–Pt(2)	57.2(1)	Pt(1)–Re–Pt(3)	54.3(1)	Re–P(7)–O(2)	120.1(3)	Re–P(7)–O(3)	122.4(3)
Pt(1)–Re–P(7)	126.6(1)	Pt(1)–Re–C(4)	133.2(3)	O(1)–P(7)–O(2)	98.4(4)	O(1)–P(7)–O(3)	101.9(3)
Pt(1)–Re–C(5)	115.6(3)	Pt(1)–Re–C(6)	61.2(3)	P(2)–P(7)–O(3)	95.9(3)	P(7)–O(1)–C(G1)	129.9(6)
Pt(2)–Re–Pt(3)	54.2(1)	Pt(2)–Re–P(7)	124.0(1)	P(7)–O(2)–C(H1)	126.3(5)	P(7)–O(3)–C(I1)	123.9(6)
Pt(2)–Re–C(4)	136.0(3)	Pt(2)–Re–C(5)	58.7(3)	P(1)–C(1)–P(2)	112.2(4)	P(3)–C(2)–P(4)	111.4(4)
Pt(2)–Re–C(6)	118.4(3)	Pt(3)–Re–P(7)	177.6(1)	P(5)–C(3)–P(6)	108.2(4)	Re–C(4)–O(4)	178.1(9)
Pt(3)–Re–C(4)	94.9(3)	Pt(3)–Re–C(5)	83.2(3)	Pt(2)–C(5)–Re	76.5(3)	Pt(2)–C(5)–O(5)	111.9(6)
Pt(3)–Re–C(6)	92.3(3)	P(7)–Re–C(4)	85.8(3)	Re–C(5)–O(5)	171.4(8)	Pt(1)–C(6)–Re	76.2(3)
P(7)–Re–C(5)	94.5(3)	P(7)–Re–C(6)	90.0(3)	Pt(1)–C(6)–O(6)	112.9(6)	Re–C(6)–O(6)	170.6(8)

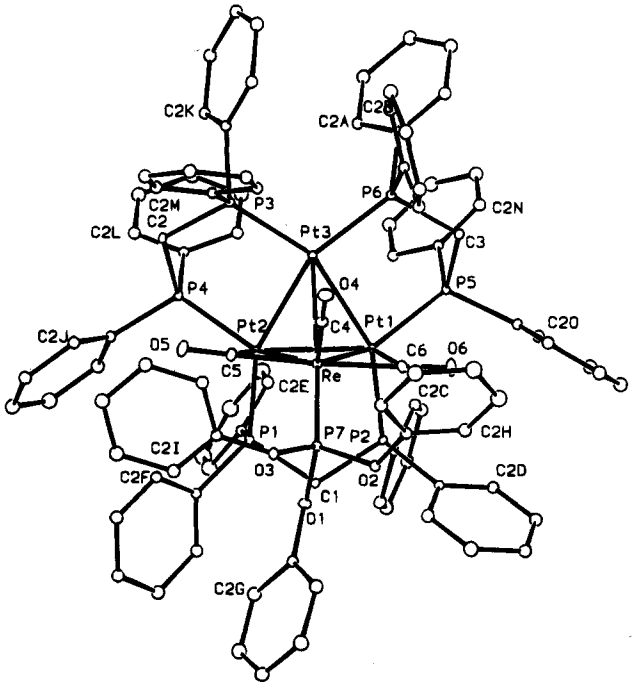

Figure 1. View of the molecular structure of **5**, with atoms represented by spheres of arbitrary size. In the phenyl rings, atoms are numbered in sequences C(n1)...C(n6), where n = A – L and the C(n1) atom is P- or O-bonded. The H atoms are omitted for clarity.

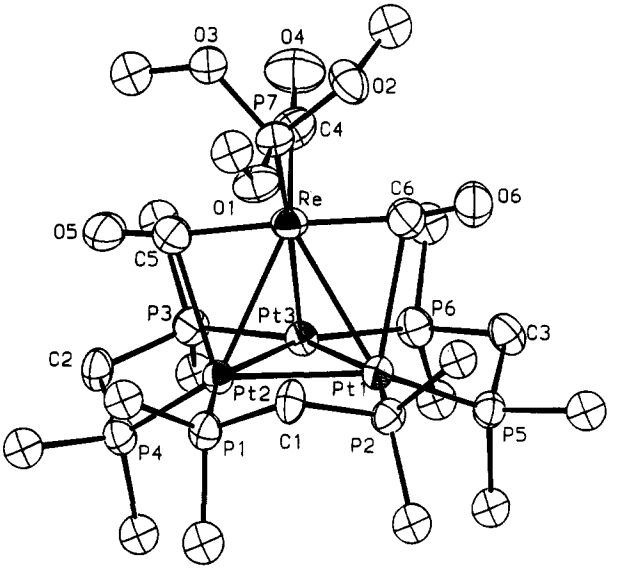

Figure 2. View of the inner core of **5**, using 50% probability ellipsoids. Only the *ipso* carbon atoms of the phenyl groups are shown.

In the $Pt_3(\mu\text{-dppm})_3$ fragment, the Pt_3P_6 skeleton is severely distorted from the ideal latitudinal geometry (Figure 2). All Pt–P bonds are bent out of the Pt_3 plane and away from the bulky $Re(CO)_3\{P(OPh)_3\}^+$ fragment. The out-of-plane displacement of the phosphorus atoms [0.088(2)–1.195(2) Å] is particularly large for the P(4) and P(5) atoms [1.195(2) and 0.969(2) Å], evidently to create space for the semibridging carbonyl ligands. The conformation of the $Pt_3P_6C_3$ unit differs from that in **2**, where the Pt_3P_6 skeleton is essentially planar and all three Pt_2P_2C rings show envelope conformations with carbon at the flap.[5] In **5** the three rings also adopt

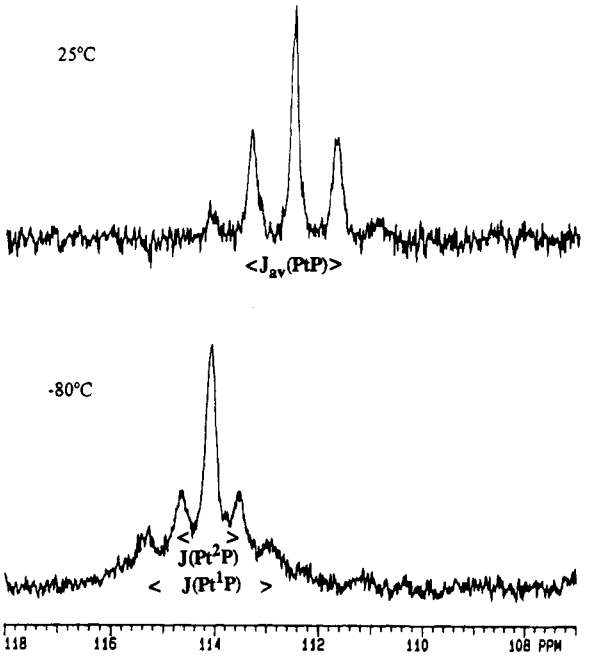

Figure 3. ^{31}P NMR spectra of complex **5** in the region of the P(OPh)$_3$ ligand. Upper, spectrum at 25 °C showing the apparent 1:4:7:4:1 quintet due to equal coupling to all platinum atoms in the fast fluxionality region. Lower, spectrum at −80 °C showing the 1:4:1 triplet of 1:8:18:8:1 quintets due to coupling to Pt^2 and 2 × Pt^1, respectively, in the slow rotation region.

envelope conformations, but with carbon at the flap only in the Pt(1)Pt(2)P(1)C(1)P(2) ring; in the other two rings the flaps are occupied by phosphorus atoms, P(4) and P(5) (Figure 2).

The spectroscopic data give further insight into the nature of the cluster cations **4** and **5**. The IR spectra of both **4** and **5** displayed three bands due to terminal carbonyls, as expected for the structure of Figure 1. The stretching frequencies were decreased slightly compared to **2**,[5] indicating that the phosphites are net donors to rhenium. The room temperature ^{31}P NMR spectra contained a singlet resonance due to the dppm phosphorus atoms and a 1:4:7:4:1 quintet for the phosphite ligand. The quintet resonance is characteristic of a nucleus with equal coupling to three platinum atoms and, together with the singlet dppm resonance, suggests that the clusters have C_3 symmetry on the NMR time scale.[8-10] Since the actual symmetry is lower (Figure 1), the clusters must be fluxional. The average coupling between platinum and the phosphite phosphorus, J(PtP), is 157 and 194 Hz for **4** and **5**, respectively. Such small couplings cannot be due to ^1J(PtP)[5,8-10] but are consistent with a longer range ^2J(PtReP) coupling, as expected if P(OR)$_3$ adds to the rhenium atom of **2**.

The apparent fluxionality of **4** and **5** was studied by low-temperature ^{31}P NMR spectroscopy. At −80 °C, the singlet dppm phosphorus resonance observed at room temperature for **5** split to give three resolved resonances. This is expected for the structure shown in eq 1, which possesses a plane of symmetry containing the atoms LRe(C^{1}O)Pt^2 (note that the atom labeling is different from that in Figure 1). Analysis of the resonance due to the phosphite ligand of **5** was also informative. At ambient temperature, this resonance appeared as a 1:4:7:4:1 quintet with ^2J(PtP) = 194 Hz (Figure 3). At −80 °C, this signal was broader and two

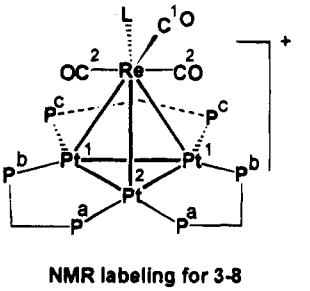

NMR labeling for 3-8

different couplings ^2J(PtP) were observed. Thus the resonance was interpreted as a 1:4:1 triplet [due to coupling to one platinum atom with ^2J(Pt^{2}P) = 300 Hz] of 1:8:18:8:1 quintets [due to coupling to two equivalent platinum atoms with ^2J(Pt^{1}P) = 135 Hz].[10] The average coupling is therefore expected to be $^1/_3$(2 × 135 + 300) = 190 Hz, in good agreement with the observed value of 194 Hz. The mechanism of fluxionality is proposed to be that shown in eq 3. It involves rotation of the

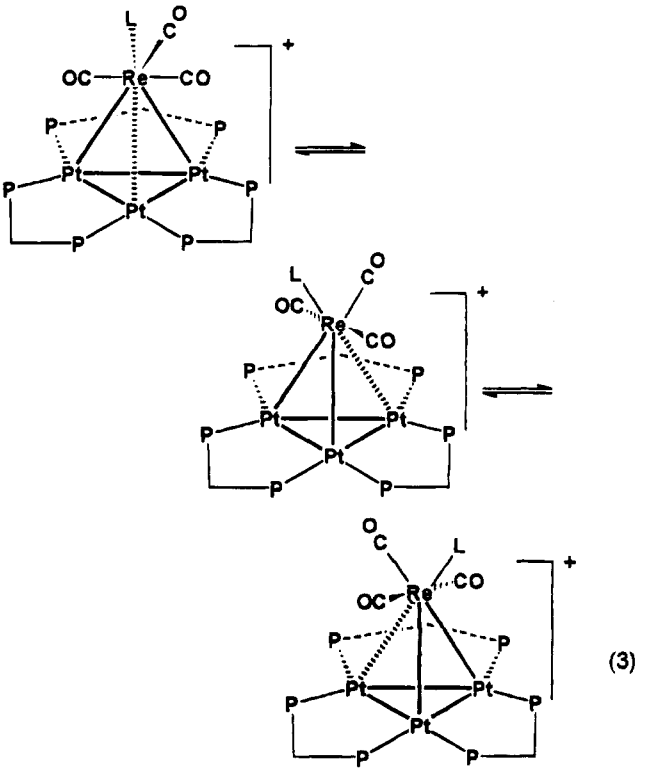

(3)

Re(CO)$_3$L unit about the Pt$_3$ triangle, with each stable structure having an approximately linear L−Re−Pt unit [P(7)−Re−Pt(3) = 177.6(1)° in Figure 1]. This naturally leads to apparent 3-fold symmetry at the limit of rapid rotation. The activation energy for rotation of the Re(CO)$_3$L unit of **4** appears to be lower than for **5**. Thus, at −80 °C, the ^{31}P resonance due to the dppm phosphorus atoms had split into three broad unresolved resonances, indicating that the fluxionality was not completely frozen out. The difference is most readily interpreted in terms of steric hindrance involving the phosphite ligand leading to slower rotation of the Re(CO)$_3$L unit when L = P(OPh)$_3$ than with the smaller L = P(OMe)$_3$.

The reaction of P(OMe)$_3$ with **3** gave a complex mixture of products, which were not identified, while P(OPh)$_3$ failed to react with **3** at room temperature.

Reactions with CO. Solutions of the tricarbonyl

Scheme 1

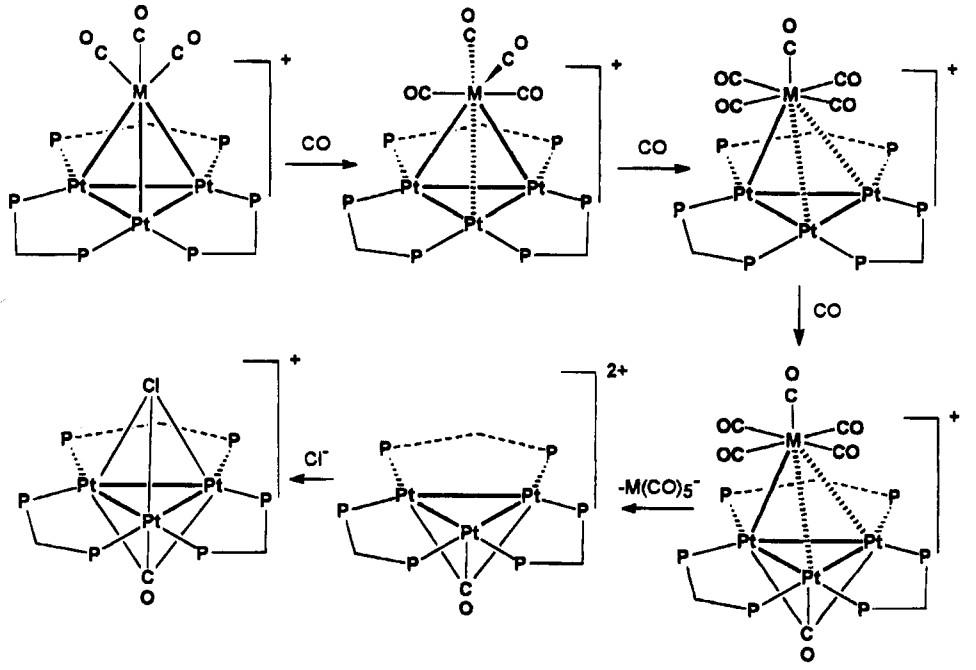

cluster cation **2** in acetone or dichloromethane reacted rapidly with CO to give the tetracarbonyl cluster $[Pt_3\{\mu_3\text{-}Re(CO)_4\}(\mu\text{-dppm})_3]^+$, **6** (eq 1). The reaction was reversible, and bubbling nitrogen through the solution containing **6** led to loss of one carbonyl ligand with formation of **2**. This reversibility gives an easy route for enrichment of the cluster with ^{13}CO and clearly indicates how ligand substitution reactions may occur at the rhenium center of **2**. Redissolution of solid samples containing **6** also gave solutions containing mixtures of **2** and **6**, so that pure samples of **6** were obtained with some difficulty. These reactions were readily monitored by NMR or IR spectroscopy. Both **2** and **6** are deep red in color, but **6** is slightly darker in color than **2**. Complex **6** was stable to excess CO in acetone solution but unstable in dichloromethane, in which further reaction occurred to give cluster fragmentation and formation of the known cluster $[Pt_3(\mu_3\text{-}Cl)(\mu_3\text{-}CO)(\mu\text{-dppm})_3]^+$;[8,13] the rhenium-containing product was not identified. Interestingly, as monitored by ^{31}P NMR spectroscopy, the fragmentation appeared to proceed via an intermediate cluster, which showed a singlet at $\delta(^{31}P)$ −23.3. The concentration of this complex grew in the early stages of reaction and then decreased as the final products were formed, so it could not be isolated. It is possible that this complex is formed by addition of a second carbonyl ligand to give $[Pt_3\{Re(CO)_5\}(\mu\text{-dppm})_3]^+$.

The reaction of the Pt_3Mn cluster **3** with CO did not give an identifiable carbonyl adduct. When the reaction was carried out in dichloromethane, the platinum cluster $[Pt_3(\mu_3\text{-}Cl)(\mu_3\text{-}CO)(\mu\text{-dppm})_3]^+$ was formed but no intermediates could be detected.[8,10] Again, the formation of this chloro complex is due to the involvement of the solvent used. However, in contrast to the reaction of **2**, when complex **3** was treated with CO in acetone, fragmentation of the cluster took place, yielding the known cluster cation $[Pt_3(\mu_3\text{-}CO)(CO)(\mu\text{-dppm})_3]^{2+}$. This is known to be formed reversibly by reaction of $[Pt_3(\mu_3\text{-}CO)(\mu\text{-dppm})_3]^{2+}$ with CO,[14] and flushing the acetone solution of $[Pt_3(\mu_3\text{-}CO)(CO)(\mu\text{-dppm})_3]^{2+}$ with dinitrogen gave rise to $[Pt_3(\mu_3\text{-}CO)(\mu\text{-dppm})_3]^{2+}$. The easier fragmentation of the Pt_3Mn cluster is indicative of a weaker Pt−Mn bond in comparison with the corresponding Pt−Re bond.

Both reactions of **2** and **3** can be understood in terms of Scheme 1. Sequential CO additions at rhenium or manganese give the tetracarbonyl and pentacarbonyl clusters, and the next addition occurs at platinum with displacement of $[M(CO)_5]^-$, M = Mn or Re. The cluster $[Pt_3(\mu_3\text{-}CO)(\mu\text{-dppm})_3]^{2+}$ is stable in dichloromethane, so the formation of $[Pt_3(\mu_3\text{-}Cl)(\mu_3\text{-}CO)(\mu\text{-dppm})_3]^+$ is probably initiated by reaction of $[M(CO)_5]^-$ with CH_2Cl_2 with generation of Cl^-. It should be clear that the reactions shown in Scheme 1 are just the reverse of those which are presumably involved in the formation of **2** or **3** from **1** and $[M(CO)_5]^-$.[5]

The new complex **6** was characterized spectroscopically. The IR spectrum contained two terminal carbonyl bands [ν(CO) = 1995, 1889 cm^{-1}], shifted to higher frequency compared to **2** [ν(CO) = 1981, 1882, 1871 cm^{-1}],[5] and no bridging carbonyl bands. The room temperature ^{31}P NMR spectrum of **6** showed a singlet, with complex satellites arising from coupling to ^{195}Pt that are typical of complexes with metal−metal-bonded $Pt_3(dppm)_3$ triangles with apparent C_3 symmetry.[6,8] The ^{13}C NMR spectrum of **6***, prepared by using ^{13}CO, was more informative. It displayed two carbonyl resonances in a 1:1 ratio, a singlet at δ 196 and a more complex resonance at δ 217. The latter resonance appears as an apparent quintet with 1:4:7:4:1 intensities, typical of a group coupled to three equivalent platinum atoms. The observed coupling constant, J(PtC) = 160 Hz, is much too low for a ^1J(PtC) coupling but is consistent with a ^2J(PtReC) coupling.[14] Clearly then, all four carbonyls are bound to rhenium but are in two different

(13) Manojlović-Muir, Lj.; Muir, K. W.; Lloyd, B. R.; Puddephatt, R. J. *J. Chem. Soc., Chem. Commun.* **1985**, 536.

(14) Lloyd, B. R.; Bradford, A. M; Puddephatt, R. J. *Organometallics* **1987**, *6*, 424.

chemical environments, with two showing long-range coupling to platinum and two not coupled to platinum. These data are mostly consistent with the proposed structure shown in eq 1 with L = CO except, of course, that such a $Re(CO)_4$ unit cannot have C_3 symmetry whereas the spectra suggest that this symmetry element is present. The problem is overcome if the cluster is fluxional, undergoing rapid rotation of the $Re(CO)_4$ group with respect to the Pt_3 triangle. To test for this, low-temperature ^{31}P and ^{13}C NMR spectra were recorded. The ^{31}P NMR spectrum of **6** at −80 °C was far broader than at room temperature, but it did not split into separate resonances. The ^{13}C NMR spectrum did not change significantly at −80 °C except that the quintet broadened and $J(PtC) = 77$ Hz was somewhat decreased. These data indicate that rotation of the $Re(CO)_4$ unit was still fairly rapid at −80 °C. The rate of rotation of the $Re(CO)_3L$ units in **4**−**6** appears to follow the sequence L = $P(OPh)_3$ < L = $P(OMe)_3$ < L = CO, as expected if the main barrier to rotation is steric hindrance.

Reactions with Isocyanides RNC (R = Me, t-Bu, Cy (cyclohexyl), Xy (2,6-$Me_2C_6H_3$)). The reactions of isocyanide ligands RNC with **2** gave the adducts $[Pt_3\{Re(CO)_3(CNR)\}(\mu\text{-dppm})_3]^+$, **7** (R = Me), **8** (R = t-Bu), **9**, (R = Cy), and **10** (R = Xy) by addition to the rhenium center. In contrast, these ligands react with equal molar amounts of the cluster $[Pt(\mu_3\text{-CO})(\mu\text{-dppm})_3]^{2+}$ to form the adducts $[Pt_3(CNR)(\mu_3\text{-CO})(\mu\text{-dppm})_3]^{2+}$ by addition at platinum.[12] The reaction of **2** with RNC took about 1/2 h (R = Me, t-Bu, Cy) or 1 h (R = Xy) to reach completion as monitored by NMR spectroscopy. The isocyanide adducts are stable in solution under a N_2 atmosphere.

The IR spectrum of **10** displayed two terminal carbonyl bands at $\nu(CO)$ = 1981 and 1874 cm^{-1} and a terminal isocyanide absorption at $\nu(NC)$ = 2088 cm^{-1}. Note that the value of $\nu(NC)$ is lower than in free XyN≡C (2115 cm^{-1}), whereas the value of $\nu(NC)$ in $[Pt_3(\mu_3\text{-CO})(XyN{\equiv}C)(\mu\text{-dppm})_3]^{2+}$ = 2165 cm^{-1} is higher, indicating stronger back-bonding to the isocyanide ligand when coordinated to rhenium. The room temperature ^{31}P NMR spectrum of **10** gave a sharp singlet resonance, but, at −90 °C, this split to give three broad resonances at δ 3.1, −3.0, and −13.1, respectively. The ^{31}P NMR spectrum coalesced at −50 °C. These data are fully consistent with fluxionality as shown in eq 3.

The spectroscopic properties of **7**−**9** are similar, and details are given in the Experimental Section. In all cases the values of $\nu(NC)$ were lower than in the free ligands (2144, 2102, and 2120 cm^{-1} for **7**−**9**, respectively, compared to 2167, 2140, and 2145 cm^{-1} for free MeNC, t-BuNC, and CyNC in CH_2Cl_2 solution, respectively), indicative of coordination to the rhenium center in all cases.

Reactions with Thiols RSH (R = Et, t-Bu or 3-MeC_6H_4). The thiol ligands RSH reacted with cluster **2** to give the adducts **11**−**13**, R = Et, t-Bu, or 3−MeC_6H_4, respectively (eq 1). The reaction rates followed the sequence R = Et (seconds to complete) > t-Bu (minutes) > 4-MeC_6H_4 (1 h), as monitored by ^{31}P NMR spectroscopy. In contrast, the thiol ligands RSH (R = Et and Ph) react with $[Pt(\mu_3\text{-CO})(\mu\text{-dppm})_3]^{2+}$ to form $[Pt_3(SHR)(\mu_3\text{-CO})(\mu\text{-dppm})_3]^{2+}$, which then readily transforms to the stable $[Pt_3H(\mu_3\text{-SR})(\mu_3\text{-CO})(\mu\text{-dppm})_3]^{2+}$.[8,12]

The IR spectrum of **13** contained three terminal carbonyl bands at $\nu(CO)$ = 1997, 1897, and 1883 cm^{-1}. The room temperature ^{31}P NMR spectrum of **13** showed a sharp singlet resonance due to the dppm ligands, with satellites due to coupling to ^{195}Pt, indicating 3-fold symmetry on the NMR time scale. The resonance broadened but did not split at −90 °C indicating a low barrier to rotation of the $Re(CO)_3(RSH)$ unit. The magnitude of coupling, $^1J(PtP)$ = 3028 Hz, is similar to those of isocyanide adducts.

Reactions with Alkynes. The reactions of alkynes also occur rapidly according to eq 1 to give the new alkyne clusters $[Pt_3\{Re(CO)_3L\}(\mu\text{-dppm})_3]^+$ (**14**, L = HC≡CH; **15**, L = PhC≡CH). These were thermally stable complexes. For example, **14** could be heated under reflux in benzene without decomposition by either CO or HC≡CH loss. The disubstituted alkynes RC≡CR, R = Me, Ph, CF_3, or CO_2Me, failed to react with **2**, presumably due to steric hindrance. The alkyne complexes failed to give X-ray quality crystals, so spectroscopic characterization was necessary. There are two possible complications with alkyne ligands. The first is that rearrangement of Re(HC≡CR) to the vinylidene Re=C=CHR is possible,[15] and the second is that two orientations of the alkyne are possible, either *in* the plane of symmetry, **A**, or *perpendicular to* the plane of symmetry of the cluster, **B**. The ^{13}C NMR spectrum of

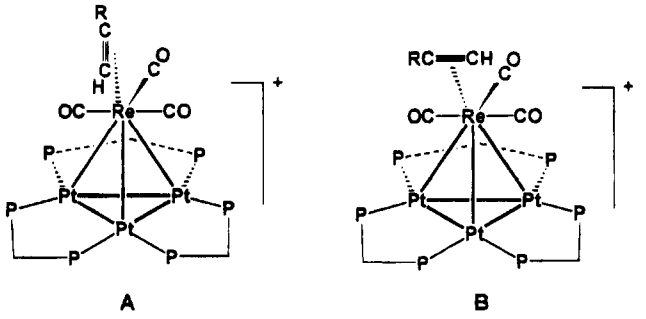

14*, prepared using ^{13}C-enriched acetylene, contained only a broad singlet, with no resolved $^{13}C-^{195}Pt$ coupling, for the coordinated acetylene at either room temperature or at −80 °C. The broadening of the peak is probably due to quadrupolar relaxation by the rhenium nucleus (^{185}Re and ^{187}Re each have $I = 5/2$). The absence of $J(PtC)$ coupling immediately shows that the alkyne is bound to rhenium and not platinum, and the presence of only one resonance at δ 85.2 immediately rules out the vinylidene structure which would give two ^{13}C resonances, of which the α-carbon resonance would be expected in the range δ 250−380.[15b] It is less certain if the conformation is **A** or **B**; only **B** should give a single ^{13}C resonance and so this is the more likely structure. However, the possibility that the structure is **A** with a rapidly rotating acetylene ligand cannot be eliminated by the data. The ^{31}P NMR spectrum of **14** contained three resonances for the dppm phosphorus atoms, and these resonances showed no significant change at temperatures from 25 to −80 °C. Hence this cluster is not fluxional and the $Re(CO)_3(HCCH)$ group cannot easily rotate with respect to the Pt_3 triangle. The ^{31}P NMR spectrum of **15** contained six resonances, showing that all six phosphorus atoms are inequivalent. In structure

(15) (a) Caulton, K. G. *Coord. Chem. Rev.* **1981**, *38*, 1. (b) Bruce, M. I. *Chem. Rev.* **1991**, *91*, 197.

A the plane of symmetry remains even with an unsymmetrical alkyne and so this should give only three ^{31}P resonances. The observation of six resonances is therefore strong evidence for structure **B**.

It is noted that alkynes react with complex **1** at the Pt_3 triangle and so give rise to very different products containing triply bridging alkyne ligands.[8,16] The reactions of HCCH and PhCCH with **3** gave an unidentified mixture of products.

Ligand Exchange Reactions. The cluster **6** can undergo ligand for carbonyl exchange according to Scheme 2 (L = CO) on reaction with ligands L′ (L′ = $P(OMe)_3$, $P(OPh)_3$, HCCH, HCCPh) by substitution at rhenium while reactions with halide (X = Cl, Br, I) lead to displacement of L = CO from rhenium with addition of X^- at platinum. These substitution reactions are all substantially slower than the analogous addition reactions to cluster **2**. Similarly, the cluster $[Pt_3\{Re(CO)_3(HCCH)\}(\mu\text{-dppm})_3]^+$, **14**, reacted slowly (ca. 14 and 24 h to completion when R = Me or Ph respectively) with $P(OR)_3$ (R = Me and Ph) by displacement of acetylene to give **4** or **5** respectively. The rates followed the sequence **2** ≫ **6** ≫ **14** in reactions with the phosphite ligands. The reactions with **14** are presumed to be associative since **14** is stable to dissociation of acetylene. Carbon monoxide did not displace acetylene from **14**.

Discussion

The cations **2** and **3** are coordinatively unsaturated 54-electron clusters.[7] The bonding in **2** has been interpreted in terms of the three filled M−M bonding orbitals of the $Pt_3(\mu\text{-dppm})_3$ fragment (a_1 + e symmetry) acting as donors to the three vacant acceptor orbitals of the $Re(CO)_3$+ fragment (also a_1 + e symmetry) as shown in **C**.[5] In this way, each Pt atom shares 16 and

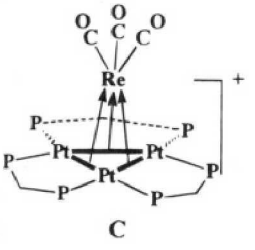

C

the Re atom shares 18 valence electrons.[5] It might be expected that ligands would therefore add selectively to platinum in much the same way as has been observed in trinuclear complexes such as $[Pt_3(\mu_3\text{-CO})(\mu\text{-dppm})_3]^{2+}$.[8] However, all the ligands studied in this work add selectively at rhenium (eq 1). It is interesting to ask why.

Consider first the bonding in the products, all of which probably have a 56-electron count (the possibility of the alkyne acting as a 4-electron donor has not been disproved). Complex **6** is the simplest example. The bonding may still be considered in terms of the $Pt_3(\mu\text{-dppm})_3$ fragment acting as a donor to the $Re(CO)_4$+ fragment, but this has only two acceptor orbitals so only

(16) Manojlović-Muir, Lj.; Muir, K. W.; Rashidi, M.; Schoettel, G.; Puddephatt, R. J. *Organometallics* **1991**, *10*, 1719.

Scheme 2

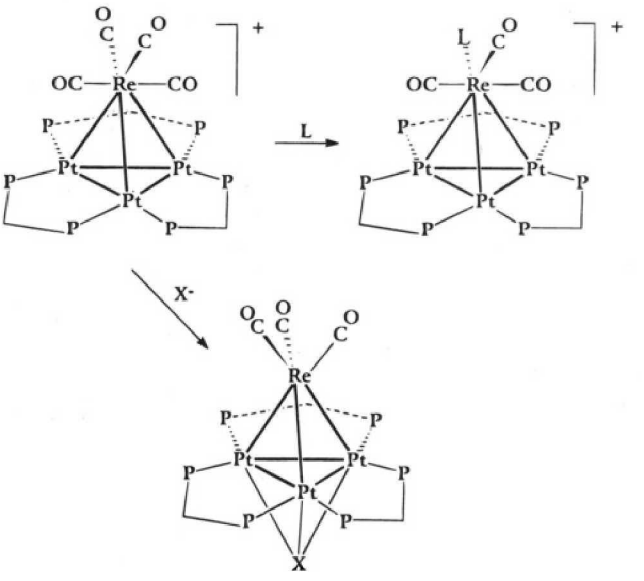

[a] L = $P(OR)_3$ or HCCH; X = Cl, Br, or I.

two donor−acceptor bonds are possible as shown in **D**.[17] Hence, weaker Pt−Re bonding is expected in **6** than in

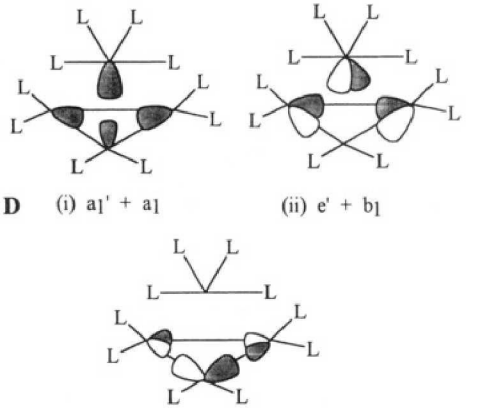

D (i) $a_1' + a_1$ (ii) $e' + b_1$ (iii) e′

2, consistent with the observed increase in Pt−Re bond distances in **5** compared to **2**. This interpretation also rationalizes the slippage of the rhenium from the center of the Pt_3 triangle in **5**. Another way of looking at this is to consider that the LUMO in **2** is a cluster antibonding orbital of e symmetry and considerable Re character. Donation of two electrons into such an orbital will naturally weaken the cluster bonding.[7] It should be pointed out that if the ligand did add below the Pt_3 plane it could donate electron density into one or more of the empty p-orbitals on platinum and this need not weaken the cluster bonding; this is what happens when ligands add to the Pt_3 cluster **1**.[8]

There is another useful analogy to this chemistry. The proposed donor orbitals of the $Pt_3(\mu\text{-dppm})_3$ fragment have a_1 + e symmetry and so do the donor orbitals of $C_5H_5^-$ or C_6H_6.[15] Hence, in the limit, it could be argued that the cluster **2** is isolobal to $[CpRe(CO)_3]$. This

(17) For previous theoretical work on Pt_3L_6 clusters and on $M(CO)_n$ fragments, see: (a) Evans, D. G. *J. Organomet. Chem.* **1988**, *352*, 397. (b) Mealli, C. *J. Am. Chem. Soc.* **1985**, *107*, 2245. (c) Albright, T. A.; Burdett, J. K.; Whangbo, M.-H. *Orbital Interactions in Chemistry*; Wiley: New York, 1985; Chapter 20.

complex is inert to ligand addition but the related complex [CpRe(CO)(NO)R] is known to add ligands at rhenium with slippage of the η^5-C_5H_5 ligand to η^3 and then η^1.[18] The ligand addition to **2** could be considered analogous to this chemistry. Hence, the addition of one or two ligands to **2** might lead to slippage of the $Re(CO)_3L_n$ unit from η^3 ($n = 0$) to η^2 ($n = 1$) and η^1 ($n = 2$) with respect to the Pt_3 triangle. The Pt_3Mn complex **3** appears to have weaker metal–metal bonding, and ligand addition appears to occur with cleavage of the manganese fragment from the cluster.

In an additional analogy, rotation of η^5-C_5H_5 ligands about the Cp–metal axis is known to occur with a very low activation energy so it might be predicted that the $Pt_3(\mu$-dppm$)_3$ "ligand" should rotate easily about the Re–Pt_3 centroid axis in **2**. There is no easy way to study this reaction which, of course, is equivalent to rotation of the $Re(CO)_3$ unit about the Pt_3 triangle. A somewhat higher activation energy might be expected for rotation of the $Re(CO)_3L$ units in **4**–**8**, since the analogy here is to η^3-Cp ligands. Nevertheless, the complexes **4**–**6** are all fluxional and only the alkyne complexes **7** and **8** are not. A related fluxionality has been observed previously for the clusters $[Pt_4(\mu\text{-H})(\mu\text{-CO})_2(\mu\text{-dppm})_3L]^+$, in which the $Pt(CO)_2L$ group migrates from edge to edge of the dppm-bridged Pt_3 triangle.[19]

The above arguments, based on analogies only, are supported by EHMO calculations on the model cluster $[Pt_3(CO)_6\{\mu\text{-Re}(CO)_4\}]^+$, substituting two carbonyl ligands for each μ-dppm ligand in **6** and with initial geometry **E**. An energy correlation diagram is shown as Figure

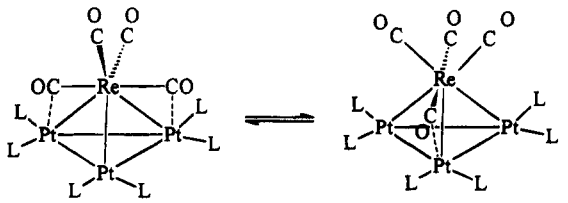

E **F**

4. The $2a_1$ acceptor orbital of the $[Re(CO)_4]^+$ fragment[17] overlaps with the $1a_1'$ donor orbital of the $[Pt_3(CO)_6]$ fragment[17] to give the bonding orbital 3a′, which is the HOMO. The $1b_1$ acceptor orbital of the $[Re(CO)_4]^+$ fragment overlaps with one of the 1e′ donor orbitals of the $[Pt_3(CO)_6]$ fragment to give the bonding orbital 2a′. Both of these effects contribute to Pt–Re bonding, and it is the $1b_1$–1e′ overlap which leads to asymmetry in the Pt–Re bonding. The other e′ donor orbital is destabilized by a four-electron interaction with one of the filled "t_{2g}-like" orbitals of the d^6 $[Re(CO)_4]^+$ fragment (note that the net repulsive interaction is also reduced by slippage of the $Re(CO)_4$ group). Rotation of the $[Re(CO)_4]^+$ fragment is calculated to have a low activation barrier, since, as overlap of $1b_1$ with one of the 1e′ donors decreases, overlap with the other increases, and the energies of the frontier orbitals change only slightly

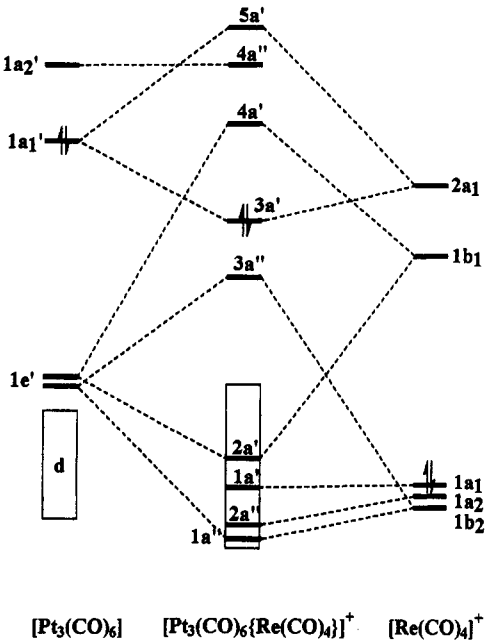

Figure 4. Energy correlation diagram for interaction of D_{3h} $[Pt_3(CO)_6]$ and C_{2v} $[Re(CO)_4]^+$ fragments to give C_s $[Pt_3(CO)_6\{Re(CO)_4\}]^+$. For frontier orbitals, see **D**.

during the rotation between limiting structures **E** and **F**. Note, however, that the rhenium is expected to move during the rotation to remain away from the center of the Pt_3 triangle. The preferred orientation may be determined by steric effects, by the semibridging carbonyl effects or by changes in energy due to slippage of the Re atom with respect to the Pt_3 triangle. The EHMO method is not well suited to geometry optimization so these effects have not been pursued, though it should be clear from the 1e′–b_1 overlap shown in **D** why the slippage of rhenium toward an edge of the Pt_3 triangle is favored.

The observation that Pt_3Re cluster **2** is reactive at the rhenium center was unexpected. It is not known what role each metal plays in the heterogeneous Pt/Re catalysts, but, on the basis of the model complex **2**, an active role for the rhenium atoms may be envisaged.[20]

Experimental Section

The compounds $[Pt_3\{M(CO)_3\}(\mu\text{-dppm})_3]^+$ (M = Re, **2**; Mn, **3**) were prepared by the previously reported procedure.[5] IR spectra were recorded by using a Perkin-Elmer 2000 spectrometer, and the NMR spectra were recorded in CD_2Cl_2 solution at ambient temperature, unless otherwise indicated, with a Varian Gemini-300 spectrometer; chemical shifts are referenced to TMS (^{1}H) and 85% H_3PO_4 (^{31}P{^{1}H}). Elemental analyses were performed by Galbraith Laboratories, Inc.

$[Pt_3\{Re(CO)_3(P(OMe)_3)\}(\mu\text{-dppm})_3][PF_6]\cdot 2CH_2Cl_2$. To a solution of **2** (30 mg) in CH_2Cl_2 (10 mL) was syringed $P(OMe)_3$ (0.1 mL). The solution immediately darkened slightly. The mixture was stirred for 15 min, the solution was concentrated, and the product was precipitated as a deep brown solid by addition of pentane and then washed with pentane and dried under vacuum. It was recrystallized from CH_2Cl_2/hexane. Yield: 70%. Anal. Calcd for $C_{83}H_{79}O_6F_6P_7Cl_2RePt_3$: C, 40.7; H, 3.2. Found: C, 40.8; H, 3.4. IR (Nujol): ν(CO)/cm^{-1} = 1943 s, 1877 m, 1856 vs. NMR in CD_2Cl_2: δ(^{1}H) 6.40 [m, H_2CP_2]; 4.72 [m, H_2CP_2]; 3.10 [d, ^3J(PH) = 17 Hz, $P(OCH_3)_3$]; δ(^{31}P) 130.5 [quin, ^2J(PtP) = 157 Hz, $P(OMe)_3$]; −5.6 [s, ^1J(PtP) =

(18) (a) Casey, C. P.; O'Connor, J. M.; Jones, W. D.; Haller, K. J. *Organometallics* **1983**, *2*, 535. (b) Bang, H.; Lynch, T. J.; Basolo, F. *Organometallics* **1992**, *11*, 40. (c) Biagioni, R. N.; Lorkovic, I. M.; Skelton, J.; Hartung, J. B. *Organometallics* **1990**, *9*, 547. (d) O'Connor, J. M.; Casey, C. P. *Chem. Rev.* **1987**, *87*, 307.

(19) Douglas, G.; Manojlović-Muir, Lj.; Muir, K. W.; Jennings, M. C.; Lloyd, B. R.; Rashidi, M.; Schoettel, G.; Puddephatt, R. J. *Organometallics* **1991**, *10*, 3927.

(20) Bond, G. C. *Chem. Soc. Rev.* **1991**, *20*, 441.

3028 Hz, ^3J(PP) = 186 Hz, dppm]; δ(^{31}P, −80 °C) 132.2 [m, ^2J(PtP) = 156 Hz]; 1.1, −2.4, −15.6 [br, dppm].

[Pt$_3${Re(CO)$_3$(P(OPh)$_3$)}(μ-dppm)$_3$][PF$_6$]. Complex **5**[PF$_6$] was prepared in a similar way except that the reagent P(OPh)$_3$ was used. It was recrystallized from CH_2Cl_2/diethyl ether. Yield: 85%. Anal. Calcd for $C_{96}H_{81}O_6F_6P_7RePt_3$: C, 48.8; H, 3.3. Found: C, 48.5; H, 3.7. IR (Nujol): ν(CO)/cm^{-1} = 1955 m, 1899 m, 1868 s. NMR in CD_2Cl_2: δ(^{1}H) 6.45 [m, H_2CP_2]; 4.75 [m, H_2CP_2]; δ(^{31}P) 111.8 [quin, ^2J(PtP) = 194 Hz, P(OPh)$_3$]; −5.5 [s, ^1J(PtP) = 3007 Hz, ^3J(PP) = 195 Hz, dppm]; δ(^{31}P, −80 °C) 114.1 [tquin, ^2J(PtP) = 300 Hz, 135 Hz, P(OPh)$_3$]; 1.3 [s, br, ^1J(PtP) = 3577 Hz, dppm], −3.7 [m, ^1J(PtP) = 2833 Hz, dppm], −16.7 [m, ^1J(PtP) = 2688 Hz, dppm].

[Pt$_3${Re(CO)$_4$}(μ-dppm)$_3$][PF$_6$]. CO was bubbled through a solution of **2** (15 mg, 0.007 mmol) in CD_2Cl_2 (0.5 mL) in an NMR tube for 1 min. The solution became slightly darker in color. NMR spectra (^{1}H and ^{31}P{^{1}H}) indicated the immediate disappearance of **1** and the quantitative formation of **6**. This reaction was reversible, as evidenced by the fact that, in the absence of CO, complex **2** was slowly regenerated at the expense of **6** in the solution. IR (CH_2Cl_2): ν(CO)/cm^{-1} = 1995 s, 1889 vs. NMR: δ(^{1}H) 6.35 [m, H_2CP_2]; 4.60 [m, H_2CP_2]; δ(^{31}P) −2.6 [s, ^1J(PtP) = 3000 Hz, ^3J(PP) = 194 Hz, dppm]; δ(^{13}C) 216.5 [quin, ^2J(PtC) = 81 Hz, C^{1}O], 195.6 [s, C^{2}O]; δ(^{31}P, −80 °C) −2.8 [br, ^1J(PtP) = 3120 Hz, dppm]; δ(^{13}C, −80 °C) 217.3 [m, ^2J(PtC) = 77 Hz, C^{1}O], 196.8 [s, C^{2}O].

Addition of CO to the CD_2Cl_2 solution of **6** for a longer period led to the complete conversion to the previously characterized complex, [Pt$_3$(μ_3-Cl)(μ_3-CO)(μ-dppm)$_3$]$^+$, within 15 min.[14]

The reaction of complex **3** with CO was carried out similarly. When the reaction was conducted in CD_2Cl_2 in an NMR tube, the formation of [Pt$_3$(μ_3-Cl)(μ_3-CO)(μ-dppm)$_3$]$^+$ was occurred rapidly and in almost quantitative yield, as monitored by NMR. When this reaction was carried out using an acetone solution, the product was [Pt$_3$(μ_3-CO)(CO)(μ-dppm)$_3$]$^{2+}$ which, upon flushing with dinitrogen, was converted to [Pt$_3$(μ_3-CO)-(μ-dppm)$_3$]$^{2+}$. Both compounds are known and they were identified by their ^{1}H and ^{31}P NMR spectra.[14]

[Pt$_3${Re(CO)$_3$(MeNC)}(μ-dppm)$_3$][PF$_6$]. To a solution of **2** (36 mg, 0.017 mmol) in acetone (15 mL) was added MeNC (0.8 μL, 0.017 mmol) via microsyringe. The color of the red solution darkened immediately. After 0.5 h of being stirred, the solution was concentrated to ca. 1 mL under vacuum. Hexane was added to precipitate the product, which was further washed with diethyl ether followed by vacuum drying to give the product as an orange-yellow powder in 87% yield. Anal. Calcd for $C_{80}H_{69}F_6NO_3P_7Pt_3Re$: C, 43.78; H, 3.17. Found: C, 43.65; H, 3.16. IR (Nujol): ν(CO)/cm^{-1} = 1981 s, 1879 vs, br; ν(NC)/cm^{-1} = 2144 s. NMR in $(CD_3)_2CO$: δ(^{1}H) 6.64 [br, 3H, H^aCP_2], 4.58 [br, 3H, H^bCP_2], 2.60 [s, 3H, CH_3]; δ(^{31}P{^{1}H}) −2.5 [s, 6P, ^1J(PtP) = 2940, ^2J(PtP) = 255, ^{3}J(PP) = 189 Hz, dppm].

[Pt$_3${Re(CO)$_3$(t-BuNC)}(μ-dppm)$_3$][PF$_6$]. The same procedure as above was followed with the use of t-BuNC instead of MeNC. The product was obtained was orange-yellow powder. Yield: 80%. Anal. Calcd for $C_{83}H_{75}F_6NO_3P_7Pt_3Re$: C, 44.57; H, 3.38. Found: C, 44.30; H, 3.25. IR (Nujol): ν(CO)/cm^{-1} = 1983 s, 1869 vs, br; ν(NC)/cm^{-1} = 2102 s. NMR in $(CD_3)_2CO$: ^{1}H, δ = 6.63 [br, 3H, H^aCP_2], 4.61 [br, 3H, H^bCP_2], 0.91 [s, 9H, C(CH_3)$_3$]; δ(^{31}P{^{1}H}) −2.1 [s, 6P, ^1J(PtP) = 2975, ^2J(PtP) = 235, ^3J(PP) = 206 Hz, dppm].

[Pt$_3${Re(CO)$_3$(CyNC)}(μ-dppm)$_3$][PF$_6$]. This was prepared similarly and isolated as an orange-yellow powder. Yield: 76%. Anal. Calcd for $C_{85}H_{77}F_6NO_3P_7Pt_3Re$: C, 45.12; H, 3.43. Found: C, 44.9; H, 3.2. IR (Nujol): ν(CO)/cm^{-1} = 1980 s, 1876 s, sh, 1869 s; ν(NC)/cm^{-1} = 2192 s. NMR in $(CD_3)_2$-CO: δ(^{1}H) 6.30 [br, 3H, H^aCP_2], 4.63 [br, 3H, H^bCP_2], 1.60−0.80 [m, 11H, C_6H_{11}]; δ(^{31}P{^{1}H}) −2.3 [s, 6P, ^1J(PtP) = 2981, ^2J(PtP) = 255, ^3J(PP) = 187 Hz, dppm].

[Pt$_3${Re(CO)$_3$(2,6-Me$_2$C$_6$H$_3$NC)}(μ-dppm)$_3$][PF$_6$]. This was prepared in a similar way except that 2,6-xylyl isocyanide was used. Yield: 82%. Anal. Calcd for $C_{87}H_{75}F_6NO_3P_7Pt_3Re$: C, 45.73; H, 3.31. Found: C, 45.68; H, 3.46. IR (Nujol): ν(CO)/cm^{-1} = 1981 s, 1874 vs, br; ν(NC)/cm^{-1} = 2088 s. NMR in $(CD_3)_2CO$: δ(^{1}H) 6.30 [m, 3H, H^aCP_2], 4.73 [m, 3H, H^bCP_2], 2.60 [s, 6H, $(CH_3)_2C_6H_3NC$]; δ(^{31}P{^{1}H}), −2.5 [s, 6P, ^1J(PtP) = 3026, ^2J(PtP) = 227, ^3J(PP) = 182, dppm]; δ(^{1}H, −90 °C) 6.09 [br, 2H, H^aCP_2], 5.31 [br, 1H, H^aCP_2], 4.84 [m, 2H, H^bCP_2], 4.55 [br, 1H, H^bCP_2]; δ(^{31}P{^{1}H}, −90 °C) 3.1 [br, 2P, dppm], −3.0 [br, 2P, dppm], 13.1 [br, 2P, dppm]; ^{31}P{^{1}H} NMR spectrum coalesced at −50 °C, δ = −2.9 [br, 6P, ^1J(PtP) = 2992 Hz, dppm].

[Pt$_3${Re(CO)$_3$(3-MeC$_6$H$_4$SH)}(μ-dppm)$_3$][PF$_6$]. To a solution of **1** (34 mg, 0.016 mmol) in acetone (15 mL) was added 3-toluenethiol (1.9 μL, 0.016 mmol) via microsyringe. The color of the red solution became more intense immediately. After 0.5 h of being stirred, the solution was concentrated to ca. 1 mL under vacuum. Hexane was added to precipitate the product, which was further washed with diethyl ether followed by vacuum drying to give the product as an orange-red powder in 85% yield. Anal. Calcd for $C_{85}H_{74}F_6O_3P_7Pt_3ReS$: C, 44.82; H, 3.27. Found: C, 45.11; H, 3.10. IR (Nujol): ν(CO)/cm^{-1} = 1997 s, 1897 s, sh, 1883 s; NMR in $(CD_3)_2CO$: δ(^{1}H) 6.28 [m, 3H, ^2J(PH) = 54, H^aCP_2], 4.67 [m, 3H, H^bCP_2]; δ(^{31}P{^{1}H}) −1.9 [s, 6P, ^1J(PtP) = 3028, ^2J(PtP) = 213, ^3J(PP) = 171, dppm]; δ(^{1}H, −90 °C 6.22 [br, 3H, H^aCP_2], 4.55 [br, 3H, H^bCP_2]; δ(^{31}P{^{1}H}, −90 °C) −2.2 [br, 6P, ^1J(PtP) = 3080 Hz, dppm].

[Pt$_3${Re(CO)$_3$(C$_2$H$_5$SH)}(μ-dppm)$_3$][PF$_6$]. This was prepared similarly. Anal. Calcd for $C_{80}H_{72}F_6O_3P_7Pt_3ReS$: C, 43.36; H, 3.28. Found: C, 43.16; H, 3.12. IR (Nujol): ν(CO)/cm^{-1} = 1979 s, 1869 s, br; NMR in $(CD_3)_2CO$: δ(^{1}H), 5.81 [m, 3H, H^aCP_2], 5.44 [m, 3H, H^bCP_2], 1.86 [quar, 2H, ^3J(HH) = 7.3, CH_2 of C_2H_5], 1.11 [t, 3H, ^3J(HH) = 7.3, CH_3 of C_2H_5]; δ(^{31}P{^{1}H}) −1.9 [s, 6P, ^1J(PtP) = 2948, ^2J(PtP) = 187, ^3J(PP) = 199, dppm].

[Pt$_3${Re(CO)$_3$(t-BuSH)}(μ-dppm)$_3$][PF$_6$]. This was prepared similarly. Anal. Calcd for $C_{80}H_{72}F_6O_3P_7Pt_3ReS$: C, 43.89; H, 3.41. Found: C, 44.17; H, 3.58. IR (Nujol): ν(CO)/cm^{-1} = 1983 s, 1876 s, br; NMR in $(CD_3)_2CO$: δ(^{1}H) 6.32 [br, 3H, H^aCP_2], 4.69 [m, 3H, H^bCP_2], 1.39 [s, 9H, CH_3]; δ(^{31}P{^{1}H}) −1.9 [s, 6P, ^1J(PtP) = 3026, ^2J(PtP) = 198, ^3J(PP) = 176 Hz, dppm].

[Pt$_3${Re(CO)$_3$(HC≡CH)}(μ-dppm)$_3$][PF$_6$]. Acetylene was bubbled through a solution of **2** (30 mg) in CH_2Cl_2 (10 mL) for 1 min, immediately causing a color change to dark brown. The mixture was stirred for 15 min, the volume was reduced to

Table 2. Crystallographic Data for [Pt$_3${Re(CO)$_3$P(OPh)$_3$}(μ-dppm)$_3$][PF6]·C$_2$H$_5$(OH), 1[PF$_6$]·C$_2$H$_5$(OH)

empirical formula	$C_{98}H_{87}F_6O_7P_8Pt_3Re$
fw	2510.0
space group	$P\bar{1}$
a, Å	13.993(1)
b, Å	17.868(1)
c, Å	19.753(2)
α, deg	88.198(7)
β, deg	87.766(7)
γ, deg	72.394(4)
V, Å^3	4702.9(7)
Z	2
F(000)	2428
D_{calcd}, g cm^{-3}	1.772
cryst dimens, mm^3	0.33 × 0.25 × 0.15
temp, °C	23
radiation	Mo Kα
wavelength, Å	0.719 73
μ(Mo Kα), cm^{-1}	59.93
abs corr factors on F	0.75 to 1.20
data collcn range, θ (deg)	2.4 to 30.5
no. of reflns in refinement [$I > 3\sigma(I)$]	14765
no. of params refined	464
R	0.0405
R_w	0.0429
observation of unit wt	1.53
largest shift/esd ratio	0.10
final difference synthesis, e Å^{-3}	−0.94 to 1.19

Table 3. Atomic Fractional Coordinates and Displacement Parameters (Å²) for Atoms in the Phenyl Groups and Solvent Molecule [C(A)–C(O6), C(1S), C(2S), and O(S)]

atom	*x*	*y*	*z*	*U*	atom	*x*	*y*	*z*	*U*
Pt(1)	0.09857(2)	0.22934(2)	0.17596(1)	0.031	C(E6)	0.0350(7)	0.0325(7)	0.4021(7)	0.095(4)
Pt(2)	0.16111(2)	0.22307(2)	0.30296(1)	0.031	C(F1)	0.2617(4)	0.0273(6)	0.3687(5)	0.044(2)
Pt(3)	0.11056(2)	0.35599(2)	0.23544(1)	0.031	C(F2)	0.3285(6)	0.0566(3)	0.4005(4)	0.050(2)
Re	0.29575(2)	0.23129(2)	0.19908(2)	0.037	C(F3)	0.4077(6)	0.0062(5)	0.4344(3)	0.066(3)
P(1)	0.16276(16)	0.09659(12)	0.32031(10)	0.037	C(F4)	0.4200(4)	−0.0734(5)	0.4366(4)	0.060(2)
P(2)	0.10266(14)	0.10006(11)	0.17144(10)	0.035	C(F5)	0.3532(6)	−0.1027(3)	0.4048(3)	0.072(3)
P(3)	0.13759(15)	0.42667(11)	0.32465(10)	0.039	C(F6)	0.2740(6)	−0.0523(6)	0.3709(3)	0.060(2)
P(4)	0.10885(15)	0.28435(13)	0.40379(11)	0.038	C(G1)	0.5118(7)	−0.0230(5)	0.2006(7)	0.051(2)
P(5)	−0.02023(15)	0.30118(12)	0.10641(1)	0.037	C(G2)	0.5040(8)	−0.0738(3)	0.2531(6)	0.078(3)
P(6)	0.03969(15)	0.43991(12)	0.14921(10)	0.040	C(G3)	0.5779(5)	−0.1446(4)	0.2611(3)	0.094(4)
P(7)	0.43879(15)	0.13469(12)	0.17581(10)	0.042	C(G4)	0.6597(6)	−0.1646(5)	0.2166(6)	0.086(3)
P(8)	0.4465(2)	0.3500(2)	0.5820(2)	0.073	C(G5)	0.6676(7)	−0.1137(3)	0.1641(5)	0.096(4)
F(1)	0.3567(7)	0.3761(6)	0.5342(5)	0.163	C(G6)	0.5937(4)	−0.0429(5)	0.1561(4)	0.074(3)
F(2)	0.3749(9)	0.3201(7)	0.6307(5)	0.192	C(H1)	0.4980(4)	0.1704(4)	0.0518(4)	0.053(2)
F(3)	0.4800(7)	0.2682(5)	0.5491(6)	0.178	C(H2)	0.4569(7)	0.1750(6)	−0.0112(3)	0.074(3)
F(4)	0.4089(8)	0.4290(6)	0.6187(6)	0.181	C(H3)	0.4746(8)	0.2265(7)	−0.0601(4)	0.112(4)
(F5)	0.5068(10)	0.3835(9)	0.5346(7)	0.253	C(H4)	0.5333(4)	0.2734(4)	−0.0461(3)	0.116(5)
F(6)	0.5314(9)	0.3269(7)	0.6283(8)	0.257	C(H5)	0.5744(7)	0.2688(7)	0.0169(3)	0.102(4)
O(1)	0.4342(4)	0.0488(3)	0.1972(3)	0.051	C(H6)	0.5568(8)	0.2173(8)	0.0658(4)	0.072(3)
O(2)	0.4785(4)	0.1174(3)	0.0979(3)	0.050	C(I1)	0.5587(9)	0.1564(7)	0.2697(2)	0.050(2)
O(3)	0.5462(4)	0.1339(3)	0.2048(3)	0.048	C(I2)	0.5710(8)	0.1028(5)	0.3230(4)	0.069(3)
O(4)	0.4107(5)	0.3448(4)	0.1554(4)	0.075	C(I3)	0.5863(4)	0.1244(4)	0.3872(4)	0.088(3)
O(5)	0.3555(4)	0.2470(4)	0.3484(3)	0.069	C(I4)	0.5894(7)	0.1995(6)	0.3981(2)	0.084(3)
O(6)	0.2423(5)	0.2316(5)	0.0479(3)	0.080	C(I5)	0.5771(7)	0.2531(4)	0.3448(4)	0.076(3)
O(S)	0.8429(14)	0.2216(11)	0.6671(10)	0.256(8)	C(I6)	0.5618(5)	0.2315(6)	0.2806(4)	0.064(3)
C(1S)[b]	0.786(2)	0.221(1)	0.730(1)	0.21(1)	C(J1)	0.1605(5)	0.2278(6)	0.4794(5)	0.045(2)
C(2S)	0.7022(14)	0.2167(11)	0.7784(9)	0.152(6)	C(J2)	0.2510(4)	0.2291(3)	0.5039(2)	0.055(2)
C(1)	0.1840(6)	0.0432(4)	0.2396(4)	0.041	C(J3)	0.2921(5)	0.1811(6)	0.5580(4)	0.064(3)
C(2)	0.1537(6)	0.3709(5)	0.4072(4)	0.043	C(J4)	0.2428(5)	0.1317(5)	0.5878(4)	0.085(3)
C(3)	0.0179(6)	0.3874(5)	0.0751(4)	0.045	C(J5)	0.1523(4)	0.1304(4)	0.5633(3)	0.097(4)
C(4)	0.3687(7)	0.3009(6)	0.1722(5)	0.056	C(J6)	0.1111(6)	0.1784(7)	0.5092(5)	0.072(3)
C(5)	0.3273(6)	0.2394(5)	0.2959(4)	0.052	C(K1)	0.0431(7)	0.5211(4)	0.3436(3)	0.044(2)
C(6)	0.2546(6)	0.2298(5)	0.1050(4)	0.051	C(K2)	−0.0386(4)	0.5251(3)	0.3864(4)	0.052(2)
C(A1)	−0.0818(6)	0.5131(5)	0.1614(6)	0.046(2)	C(K3)	−0.1159(5)	0.5944(3)	0.3915(4)	0.065(3)
C(A2)	−0.1334(4)	0.5129(6)	0.2223(5)	0.051(2)	C(K4)	−0.1116(6)	0.6598(3)	0.3539(5)	0.066(3)
C(A3)	−0.2280(6)	0.5650(4)	0.2322(3)	0.069(3)	C(K5)	−0.0299(3)	0.6558(3)	0.3112(3)	0.075(3)
C(A4)	−0.2711(6)	0.6174(4)	0.1811(5)	0.077(3)	C(K6)	0.0474(6)	0.5865(3)	0.3060(5)	0.060(2)
C(A5)	−0.2195(4)	0.6176(5)	0.1201(4)	0.074(3)	C(L1)	−0.0248(6)	0.3267(5)	0.4235(6)	0.043(2)
C(A6)	−0.1248(7)	0.5655(3)	0.1103(4)	0.065(3)	C(L2)	−0.0587(5)	0.3443(7)	0.4894(5)	0.063(3)
C(B1)	0.1234(4)	0.4936(5)	0.1115(3)	0.049(2)	C(L3)	−0.1580(7)	0.3854(5)	0.5027(3)	0.081(3)
C(B2)	0.1088(7)	0.5713(3)	0.1262(6)	0.065(3)	C(L4)	−0.2234(6)	0.4089(4)	0.4501(5)	0.084(3)
C(B3)	0.1809(7)	0.6068(4)	0.1070(4)	0.084(3)	C(L5)	−0.1894(6)	0.3914(6)	0.3843(4)	0.078(3)
C(B4)	0.2676(4)	0.5645(4)	0.0731(3)	0.082(3)	C(L6)	−0.0902(8)	0.3503(4)	0.3710(4)	0.057(2)
C(B5)	0.2822(7)	0.4868(3)	0.0584(5)	0.076(3)	C(M1)	0.2536(4)	0.4554(5)	0.3185(4)	0.044(2)
C(B6)	0.2101(8)	0.4513(4)	0.0776(4)	0.063(3)	C(M2)	0.3021(5)	0.4653(3)	0.3755(3)	0.060(2)
C(C1)	−0.0110(4)	0.0692(5)	0.1845(4)	0.042(2)	C(M3)	0.3848(6)	0.4921(6)	0.3691(3)	0.071(3)
C(C2)	−0.1030(5)	0.1244(3)	0.1753(3)	0.055(2)	C(M4)	0.4191(4)	0.5089(4)	0.3057(3)	0.073(3)
C(C3)	−0.1900(5)	0.1045(5)	0.1878(5)	0.070(3)	C(M5)	0.3706(5)	0.4990(4)	0.2487(2)	0.067(3)
C(C4)	−0.1850(4)	0.0293(4)	0.2096(3)	0.069(3)	C(M6)	0.2878(7)	0.4722(7)	0.2551(3)	0.053(2)
C(C5)	−0.0930(5)	−0.0260(3)	0.2188(4)	0.077(3)	C(N1)	−0.1482(6)	0.3447(4)	0.1399(6)	0.041(2)
C(C6)	−0.0060(5)	−0.0060(5)	0.2063(6)	0.064(3)	C(N2)	−0.2180(6)	0.3973(4)	0.1004(3)	0.062(2)
C(D1)	0.1604(8)	0.0488(4)	0.0943(4)	0.040(2)	C(N3)	−0.3161(4)	0.4267(6)	0.1238(5)	0.080(3)
C(D2)	0.1007(6)	0.0428(5)	0.0421(6)	0.055(2)	C(N4)	−0.3445(5)	0.4035(4)	0.1868(5)	0.085(3)
C(D3)	0.1440(6)	0.0067(6)	−0.0171(4)	0.067(3)	C(N5)	−0.2747(5)	0.3509(4)	0.2263(3)	0.080(3)
C(D4)	0.2469(7)	−0.0234(4)	−0.0240(4)	0.064(3)	C(N6)	−0.1766(5)	0.3215(6)	0.2029(6)	0.051(2)
C(D5)	0.3067(5)	−0.0173(5)	0.0282(5)	0.087(3)	C(O1)	−0.0414(9)	0.2569(6)	0.0270(3)	0.045(2)
C(D6)	0.2634(7)	0.0188(7)	0.0874(3)	0.071(3)	C(O2)	−0.1236(7)	0.2303(3)	0.0213(4)	0.057(2)
C(E1)	0.0442(6)	0.0903(5)	0.3566(6)	0.049(2)	C(O3)	−0.1340(5)	0.1918(5)	−0.0361(3)	0.074(3)
C(E2)	−0.0397(4)	0.1500(4)	0.3380(3)	0.062(3)	C(O4)	−0.0622(7)	0.1798(5)	−0.0879(3)	0.077(3)
C(E3)	−0.1329(6)	0.1519(6)	0.3648(6)	0.095(4)	C(O5)	0.0200(6)	0.2064(3)	−0.0822(4)	0.074(3)
C(E4)	−0.1422(6)	0.0941(5)	0.4103(5)	0.108(4)	C(O6)	0.0304(6)	0.2449(6)	−0.0248(3)	0.058(2)
C(E5)	−0.0583(5)	0.0344(5)	0.4289(4)	0.114(5)					

[a] U is the isotropic displacement parameter, and for other atoms $U = {}^1/_3 \sum_{i=1}^{3}\sum_{j=1}^{3} U_{ij} a_i^* a_j^* (\vec{a}_i \cdot \vec{a}_j)$. [b] Atoms in the solvent molecule are labeled by S.

about 2 mL, followed by precipitation of the product as a dark brown solid using pentane. It was washed with pentane, dried under vacuum, and recrystallized from CH_2Cl_2/diethyl ether. Yield: 90%. Anal. Calcd for $C_{80}H_{68}O_3F_6P_7RePt_3$: C, 44.1; H, 3.2. Found: C, 43.9; H, 2.8. IR (Nujol): ν(CO)/cm^{-1} = 1979 s, 1886 s, 1867 s. NMR in CD_2Cl_2: δ(^{1}H) 6.00 [br, 2H, H_2C_2]; 5.87 [br, H_2CP_2]; 4.95 [br, H_2CP_2]; 3.92 [m, H_2CP_2]; δ(^{31}P) 25.2 [m, ^1J(PtP) = 3073 Hz, dppm], −1.1 [m, ^1J(PtP) = 2462 Hz, dppm], −15.3 [m, ^1J(PtP) = 4567 Hz, dppm]; δ(^{13}C) 85.2 (br, H_2C_2).

[Pt$_3${Re(CO)$_3$(PhC≡CH)}(μ-dppm)$_3$][PF$_6$]·CH$_2$Cl$_2$. This was prepared in a similar way except that the reagent phenylacetylene (0.2 mL) was used. The complex was recrystallized from CH_2Cl_2/diethyl ether. Yield: 70%. Anal. Calcd for $C_{87}H_{74}O_3F_6P_7Cl_2RePt_3$: C, 44.6; H, 3.1. Found: C, 44.9; H, 3.2%. IR (Nujol): ν(CO)/cm^{-1} = 1977 vs, 1882 s, 1863 s. NMR in CD_2Cl_2: δ(^{1}H) 5.50 [br, 1H, PhC$_2$*H*]; 5.18 [m, 2H, H_2CP_2]; 4.31 [m, 2H, H_2CP_2]; 3.88 [m, 2H, H_2CP_2]; δ(^{31}P) 21.3 [m, ^1J(PtP) = 3037 Hz, dppm], 13.9 [m, ^1J(PtP) = 3100 Hz, dppm], −0.4 [m, ^1J(PtP) = 2575 Hz, dppm]; −6.3 [m, ^1J(PtP)

= 2502 Hz, dppm], −16.9 [m, ^1J(PtP) = 4494 Hz, dppm], −20.5 [m, ^1J(PtP) = 4494 Hz, dppm].

Reactions of [Pt$_3${Re(CO)$_4$}(μ-dppm)$_3$][PF$_6$]. To a solution of **6** (28 mg, 0.013 mmol) in acetone (0.5 mL) was added Et_4NBr (2.7 mg, 0.013 mmol). A brown precipitate formed immediately with the evolution of CO. This precipitate was further washed with acetone (0.5 mL) to give [Pt$_3$(μ_3-Br){Re(CO)$_3$}(μ-dppm)$_3$] as a red brown powder, identified by its NMR and IR spectra. Yield: 70%. Similar reactions of **6** with Et_4NCl and Bu_4NI give complexes [Pt$_3$(μ_3-Cl){Re(CO)$_3$}(μ-dppm)$_3$] in 55% yield and [Pt$_3$(μ_3-I){Re(CO)$_3$}(μ-dppm)$_3$] in 80% yield, respectively.

Similarly, reaction of **6** (35 mg, 0.016 mmol) in acetone (15 mL) with P(OMe)$_3$ (1.9 μL, 0.016 mmol) gave [Pt$_3${Re(CO)$_3$(P(OMe)$_3$)}(μ-dppm)$_3$][PF$_6$] in 88% yield. The product was characterized by its NMR and IR spectra. Similar reactions with P(OPh)$_3$, HCCH and PhCCH afforded [Pt$_3${Re(CO)$_3$(P(OPh)$_3$)}(μ-dppm)$_3$][PF$_6$] in 85% yield, [Pt$_3${Re(CO)$_3$(HCCH)}(μ-dppm)$_3$][PF$_6$] in 90% yield and [Pt$_3${Re(CO)$_3$(PhCCH)}(μ-dppm)$_3$][PF$_6$] in 87% yield, respectively. Reactions of [Pt$_3${Re(CO)$_3$(HCCH)}(μ-dppm)$_3$][PF$_6$] with P(OMe)$_3$ or P(OPh)$_3$ to give [Pt$_3${Re(CO)$_3$(P(OMe)$_3$)}(μ-dppm)$_3$][PF$_6$] or [Pt$_3${Re(CO)$_3$(P(OPh)$_3$)}(μ-dppm)$_3$][PF$_6$] were carried out in a similar way.

X-ray Crystal Structure Analysis of 5[PF$_6$]·EtOH. The crystal was a red chunk of approximate dimensions 0.33 × 0.25 × 0.15 mm^3. The X-ray crystallographic measurements were made at 23 °C, with graphite-monochromated Mo K$_\alpha$ radiation and an Enraf-Nonius CAD4 diffractometer.

The unit cell constants (Table 2) were determined by a least-squares treatment of 25 reflections with Bragg angles 20.8 < θ < 22.9°. The intensities of diffracted beams were measured by continuous $\theta/2\theta$ scans of width (0.99 + 0.59 tan θ)° in θ. The scan speeds were adjusted to give $\sigma(I)/I$ < 0.03, subject to a time limit of 30 s. Intensities of three reflections, remeasured every 2 h, decreased by 21% of their mean initial value during the data collection. The intensities of all reflections, derived in the usual manner (q = 0.03),[21] were corrected for Lorentz, polarization, and crystal decomposition effects. The absorption correction was made at the end of isotropic refinement, using the empirical correction of Walker and Stuart.[22] The 6187 symmetry-related reflections were averaged to obtain 2999 independent ones and R(merge) = 0.031. Of 28 429 unique reflections measured, only 14 765 with $I > 3\sigma(I)$ were used in the structure analysis.

The positions of the platinum and rhenium atoms were determined from a Patterson function and those of the remaining non-hydrogen atoms from the subsequent difference Fourier syntheses. Hydrogen atoms were included in the structural model in calculated positions, and their displacement parameters were fixed at U(H) = 1.2 U(C), where U(C) is the equivalent isotropic displacement parameter of the carbon atom to which the hydrogen is bonded. No allowance was made for scattering of the hydrogen atoms of the solvent molecule. The structure was refined by full-matrix least-squares, minimizing the function $\Sigma w(|F_o| - |F_c|)^2$, where $w = \sigma|F_o|^{-2}$. The carbon and hydrogen atoms of each phenyl group were treated as a rigid body with D_{6h} symmetry, C−C = 1.38 Å and C−H = 0.96 Å. The carbon and oxygen atoms of the phenyl groups and solvent molecule were refined with isotropic displacement parameters, and the remaining non-hydrogen atoms with anisotropic displacement parameters. The atomic scattering factors and anomalous dispersion corrections were taken from the *International Tables for X-ray Crystallography*.[23] The refinement of the structure, involving 464 variables and 14 765 reflections with $I > 3\sigma(I)$, converged at R = 0.0405 and R_w = 0.0429. The residual electron density showed no chemically significant features. The final atomic coordinates and atomic displacement parameters are listed in Table 3. All calculations were performed using the GX program package.[24]

EHMO Calculations. These were carried out using the program CACAO. The geometry used was based on a planar D_{3h} [Pt$_3$(CO)$_6$] unit with d(Pt−Pt) = 2.6 Å and d(Pt−C) = 2.0 Å. The [Re(CO)$_4$]$^+$ unit was based on an octahedral fragment with d(Pt−Re) = 2.7 Å and d(Re−C) = 2.0 Å.

Acknowledgment. We thank the NSERC (Canada) for financial support, SERC (U.K.) for an equipment grant, and the Iranian government for a studentship (to A.A.T.).

Supporting Information Available: Tables giving H atom coordinates, anisotropic displacement parameters, and bond lengths and angles (6 pages). Ordering information is given on any current masthead page.

OM9502852

(21) Manojlović-Muir, Lj.; Muir, K. W. *J. Chem. Soc., Dalton Trans.* **1974**, 2427.
(22) Walker, N.; Stuart, D. *Acta Crystallogr.* **1983**, *A39*, 158.
(23) *International Tables for X-ray Crystallography*; Kynoch Press: Birmingham, U.K., **1974**; Vol. IV.
(24) Mallinson, P. R.; Muir, K. W. *J. Appl. Crystallogr.* **1985**, *18*, 51.